Modification of WO_3 thin films by MeV N^+-ion beam irradiation

2007 J. Phys.: Condens. Matter 19 186204

(http://iopscience.iop.org/0953-8984/19/18/186204)

IOP PUBLISHING JOURNAL OF PHYSICS: CONDENSED MATTER

J. Phys.: Condens. Matter **19** (2007) 186204 (9pp) doi:10.1088/0953-8984/19/18/186204

Modification of WO_3 thin films by MeV N^+-ion beam irradiation

R Sivakumar[1,5], C Sanjeeviraja[2], M Jayachandran[3], R Gopalakrishnan[4], S N Sarangi[1], D Paramanik[1] and T Som[1,6]

[1] Institute of Physics, Sachivalaya Marg, Bhubaneswar 751 005, India
[2] Department of Physics, Alagappa University, Karaikudi 630 003, India
[3] ECMS Division, Central Electrochemical Research Institute, Karaikudi 630 006, India
[4] Department of Physics, Anna University, Chennai 600 025, India

E-mail: tsom@iopb.res.in

Received 31 January 2007, in final form 1 March 2007
Published 4 April 2007
Online at stacks.iop.org/JPhysCM/19/186204

Abstract

In this paper, we report on modification of the structural, optical, vibrational, and surface morphological properties of 2 MeV N^+-ion irradiated WO_3 thin films at different fluences (up to 1×10^{15} ions cm^{-2}). Although we observe irradiation induced grain growth, no structural phase transition takes place in the WO_3 films. These are accompanied by a systematic reduction in the optical band gap of the films. These observations are corroborated by our independent micro-Raman and optical absorption spectroscopy studies. We have made an attempt to correlate these results with MeV ion–matter interaction.

(Some figures in this article are in colour only in the electronic version)

1. Introduction

Tungsten trioxide (WO_3) is a transition metal oxide and has a wide band gap. WO_3 exhibits interesting optical properties, which are important in the view of the recent interest in filters, solid-state micro-batteries, and mirrors [1, 2]. It also has important applications in flat panel display devices, gas sensors, and optical smart windows [3–5]. Electrochromic windows with an active electrochromic layer of thin WO_3 show improvements in both energy efficiency and comfort within buildings and vehicles by reducing unwanted solar heating and glare. WO_3 has the ReO_3-type crystal structure which is composed of a network of corner-shared WO_6 octahedron units [4]. These octahedron units are capable of forming clusters having different types of structures: (a) closed, spatial dense-packed structure, (b) closed, planar dense-packed structure, and (c) open chain-like structure composed of the ring-membered 3, 4, 5, and 6

[5] Present address: Department of Chemical Engineering, National Taiwan University, Taipei 10617, Taiwan.
[6] Author to whom any correspondence should be addressed.

octahedrons. In addition, reflectance and hence emittance modulation is also possible in crystalline tungsten oxide at thermal wavelengths, creating possibilities for the development of smart infrared devices with applications in areas such as the temperature control of satellites, where radiative heat transfer is the prime mechanism [4]. Several growth techniques such as electron-beam evaporation [6], sputtering [7], and pulsed laser deposition [8] are typically employed for deposition of WO_3 films. At present, the modification of structural and optical properties of WO_3 films under different conditions is a matter of intense research. These include heating, direct current injection, ultraviolet (UV) irradiation, exposure to atomic hydrogen or molecular hydrogen gas in contact with a catalyst, and irradiation by a beam of ions or electrons [4].

Ion irradiation is a useful tool for impurity doping and defect production in materials, which help to alter their structural, optical, magnetic, and vibrational properties with a high spatial selectivity [9–11]. Irradiation induced changes brought into the surface morphology of materials also play a significant role in the case of device fabrication. As far as WO_3 films are concerned, the majority of studies have focused on irradiation induced enhancement in the electrical conductivity of WO_3 films [7, 8, 12]. On the other hand, Wagner *et al* studied the N^+-ion induced enhancement in the refractive index and vibrational properties of WO_3 thin films [13]. Therefore, a lot more needs to be done to understand the effects of ion irradiation on the optical energy band gap and surface modification of thin WO_3 films. These studies will be extremely useful in assessing the viability of using WO_3 thin film based devices in radiation-harsh environments for extra-terrestrial applications.

In this paper, we report on 2 MeV N^+-ion induced changes in the structural, optical, vibrational, and surface morphological properties of electron-beam-evaporated WO_3 thin films. For this purpose, we have used complementary characterization techniques such as x-ray diffraction (XRD), optical absorption spectroscopy, micro-Raman spectroscopy, and atomic force microscopy (AFM), and have made an attempt to correlate these data. We observe irradiation induced grain growth, a reduction in the optical band gap, a reduction in the Raman peak intensities, and an increase in the surface roughness. The results are attributed to irradiation induced defect production.

2. Experiment

WO_3 thin films were grown on clean Corning 7059 microscopic glass substrates by electron-beam evaporation of pelletized WO_3 powder (99.99%) under a chamber pressure of 1×10^{-5} mbar at room temperature (RT). The thickness of the deposited film was in the range $\sim$0.6 μm. The as-deposited (pristine) WO_3 films are optically transparent, indicating that they are at or close to the desired stoichiometry. This inference is corroborated by our independent x-ray photoelectron spectroscopic analysis [6]. The films were uniformly irradiated by 2 MeV N^+ ions (with a beam size of 1×1 cm^2) at room temperature (RT) with fluences of 1×10^{13}, 1×10^{14}, and 1×10^{15} ions cm^{-2}. All the samples were irradiated under a secondary-electron suppressed geometry. In order to minimize the irradiation induced sample heating, the fluxes of the incident ions were kept low ($<10^{10}$ ions cm^{-2} s^{-1}). Monte Carlo SRIM-2003 simulation [14] predicts the projected range of the N^+ ions in the WO_3 films to be 1500 nm and hence the ions are expected to penetrate deep into the substrate. The electronic and nuclear energy losses, S_e and S_n, in WO_3 films corresponding to the 2 MeV N^+-ions are 1.6×10^{-2} and 1.2×10^{-4} keV nm^{-1}, respectively, as obtained from SRIM calculations. Since the electronic energy loss is two orders of magnitude larger than the nuclear energy loss, the incident N^+ ions lose energy predominantly via inelastic collisions with the target electrons.

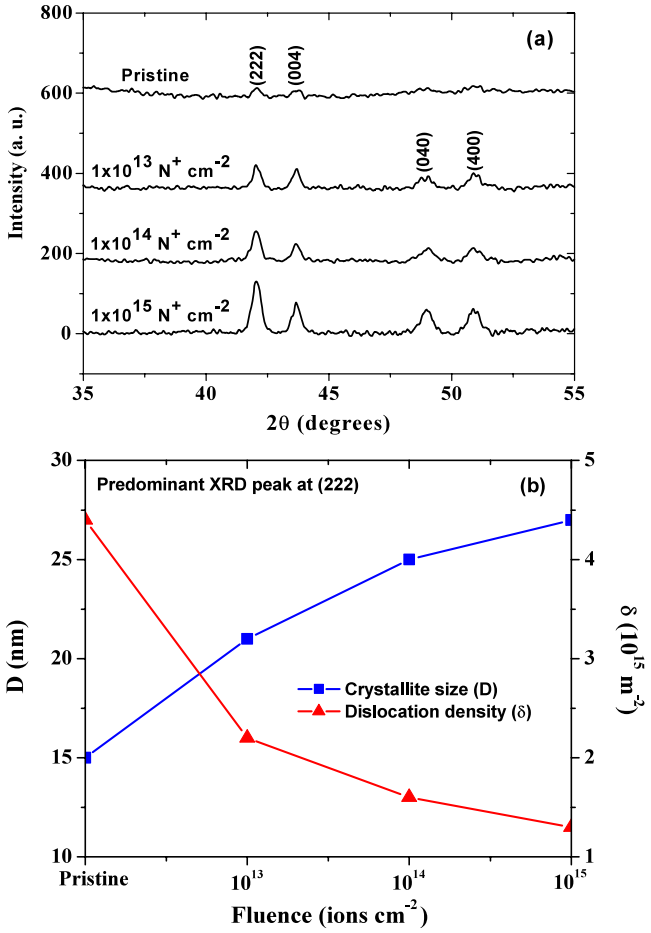

Figure 1. (a) X-ray diffraction patterns of WO_3 films before and after 2 MeV nitrogen ion irradiation at various fluences and (b) variation in the crystallite size (D) and the dislocation density (δ) versus N^+-ion fluence for WO_3 films.

Irradiation induced changes in the WO_3 films were studied by XRD using Cu Kα radiation ($\lambda = 0.154$ nm) over a 2θ scan range of 35°–55°. Changes in the optical properties of the WO_3 films before and after N^+-ion irradiation were studied by an ultraviolet–visible–near-infrared (UV–vis–NIR) spectrophotometer in the range 300–1000 nm. Micro-Raman measurements were performed at RT using a 10 μm spot size of an Ar^+-ion laser ($\lambda = 514.5$ nm) with a power of 200 mW. The spectra were collected in the range 200–1000 cm^{-1} using a backscattering geometry and a LN_2-cooled CCD. Irradiation induced changes in the surface morphology of the films were studied by AFM with a silicon nitride cantilever operated in tapping mode.

3. Results and discussion

3.1. Structural studies

XRD patterns of the pristine and the irradiated WO_3 films are shown in figure 1(a). It is seen from the XRD pattern of the pristine WO_3 film that the intensity of the peaks is very low

and they are broad as well, which suggests that the film consists of very small crystallites. The crystalline nature of the films is clearly evident from the XRD patterns of the irradiated WO_3 films, and the observed d-spacings match closely to the monoclinic phase [15]. We also do not observe any structural phase transition to take place in the films due to irradiation up to the highest fluence of 1×10^{15} ions cm^{-2}. It can be mentioned that Miyakawa *et al* [8] reported a monoclinic-to-tetragonal phase transformation in WO_3 films by either proton or helium implantation. They also reported that the critical fluence for phase transformation differs for H^+ and He^+ ion implantations, namely 2×10^{17} and 1×10^{17} ions cm^{-2} respectively [8]. In the present case, comparison with the JCPDS data shows that only a small change takes place in the lattice parameters ($a = 0.730$ nm, $b = 0.770$ nm, and $c = 0.772$ nm) of the WO_3 films irradiated up to the highest fluence [15]. Such a negligible change in the lattice parameters implies only a slight distortion in the W–O framework upon N^+-ion irradiation. On the other hand, the increasing peak intensity and narrowing of the peaks could be indicative of irradiation induced grain growth. This is clearly observed from figure 1(b) as an increase in the average crystallite size (D) and the decreasing dislocation density (δ) of the predominant peak [(222)] with increasing ion fluence. It can be mentioned here that D is defined as $0.94\lambda/\beta \cos\theta$ (Scherrer formula) [16], where β is the full width at half maximum (in radians) of the XRD peak and δ is defined as $1/D^2$ [17]. In addition, according to the theory of kinematical scattering, x-ray diffraction peaks get broadened either when crystallites become smaller than about a micrometer or if lattice defects are present in large enough abundance [18]. The observed broad peak of the pristine sample (figure 1(a)) confirmed the smaller crystallite size, as reported in figure 1(b). Normally, during ion irradiation, two competing processes occur simultaneously: one is the generation of vacancies, agglomeration of vacancies and then collapse into dislocation loops; the other is their annihilation at the possible sinks. With increasing ion fluence, though more vacancies are created, the annihilation rate of vacancies also increases as the sink density increases with irradiation. Hence, a decrease in dislocation density was observed with an increase in the ion fluence.

3.2. Optical absorption studies

Figure 2 shows the optical absorption spectra of WO_3 films before and after nitrogen ion irradiation. The absorption spectra obtained from the irradiated films show the interference pattern with a sharp increase in absorption at the band edge, which indicates the good crystallinity of the films. It is clearly seen that there is an increase in optical absorption with increasing ion fluence, which is caused by free-carrier absorption corresponding to an increase in the conductivity [19, 20]. One can also observe from these spectra (figure 2) that the absorption edges shift towards higher wavelengths, indicating a systematic reduction in the optical band gap (E_g) of the films with increasing ion fluence (inset). It may be mentioned that intrinsic absorption in a semiconductor occurs in the vicinity of its energy band gap. In addition, the fundamental absorption edge of semiconductors corresponds to the threshold for charge transitions between the highest nearly filled band and the lowest nearly empty band. The optical absorption coefficient, α is related to the energy band gap and is given by the equation [21]:

$$\alpha h\upsilon = B(h\upsilon - E_g)^n,$$

where B is a constant and E_g is the optical energy band gap. The exponent n has the values 0.5 and 2 for direct and indirect band gap, respectively. It is clearly seen from the above equation that the fundamental energy band gap depends on the variation in the optical absorption coefficient. Hence it is concluded that the red-shift in the optical absorption edge due to the ion induced effect causes the variation in energy band gap of the films.

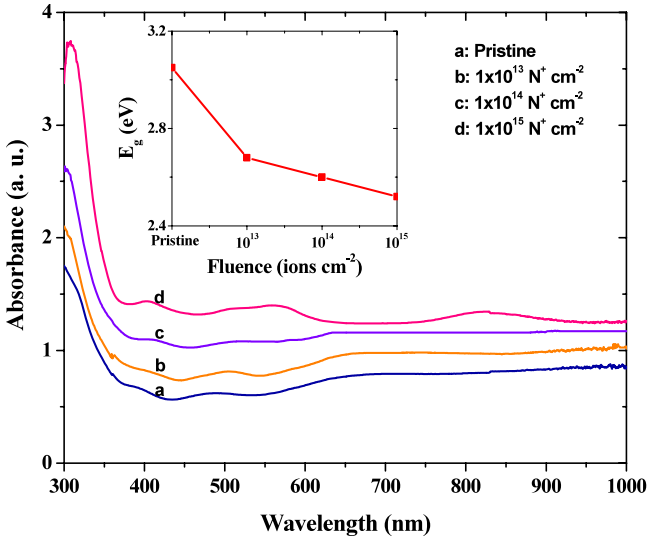

Figure 2. Optical absorption spectra of the WO_3 films before and after nitrogen irradiation at different fluences. The inset shows the variation in the energy band gap of WO_3 films with ion fluence.

Normally, WO_3 is an indirect band gap system and hence the plot of $(\alpha h\upsilon)^{1/2}$ versus $h\upsilon$ ('Tauc plot') is expected to show linear behaviour in the higher-energy region which corresponds to a strong absorption near the absorption edge. Extrapolating the linear portion to the zero absorption edge results in the optical energy band gap of the films. It is obvious that high-energy ion irradiation produces point defects such as vacancies, antisite defects and interstitials, causing lattice damage. Hence, the reduction in band gap with increasing ion fluence may arise due to the effect of band tailing, owing to the defects produced during irradiation. In fact, the high-energy ions excite the electrons from both the lone pair and bonding states to the higher-energy states. Vacancies created in these states are immediately filled by the outer electrons with Auger processes that, in turn, induce more holes in the lone pair and bonding orbital, leading to a vacancy cascade process. The vacancies occupied by electrons act as donor centres, which are responsible for broad band absorption. These donor centres are in the forbidden gap and form a narrow donor band at about 0.3 eV below the conduction band. Thus, N-ion induced defects give rise to localized states near the band edges and, as a consequence, the energy gap (3.05 eV) of the pristine sample becomes modified. This modification is presumably associated with the lowering of the conduction band edge and pushing up of the valence band edge symmetrically, which is attributed primarily to the Moss–Burstein shift in semiconductors. This leads to a decrease in the optical band gap of the irradiated WO_3 films, as shown in inset of figure 2. The inset shows that the observed band gap values are 2.68, 2.60, and 2.52 eV, respectively, corresponding to the fluences of 1×10^{13}, 1×10^{14}, and 1×10^{15} ions cm^{-2}, respectively.

3.3. Vibrational and surface morphological properties

The Raman spectra of the pristine and the irradiated WO_3 films are shown in figure 3. As mentioned earlier, WO_3 consists of a network of corner-shared WO_6 octahedra units, which are capable of forming clusters. These clusters are supposed to be connected to each other

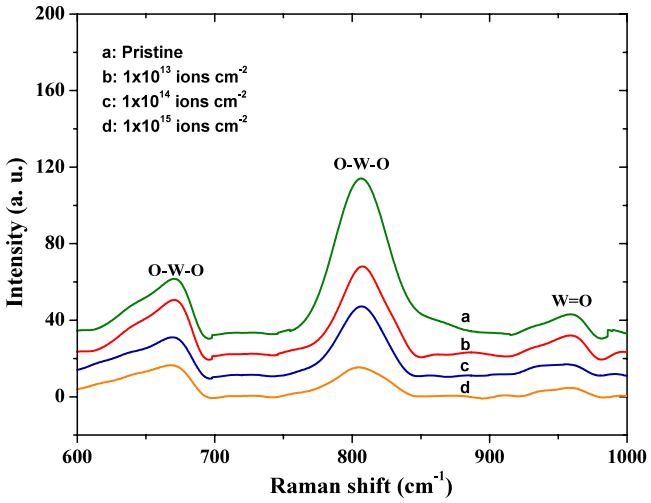

Figure 3. Micro-Raman spectra of the WO_3 films before and after N^+-ion irradiation at various fluences.

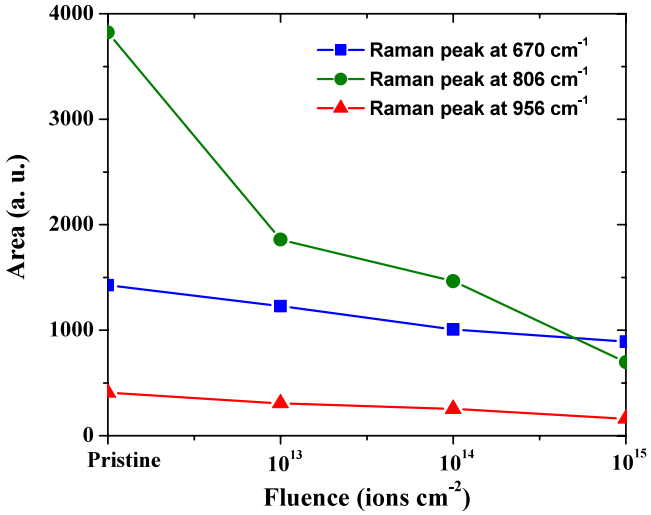

Figure 4. Variation in the Raman peak areas of the WO_3 films with N^+-ion fluence.

by O–W–O grains with terminal W=O bonds at the boundaries [22, 23]. The observed broad peaks at 670 and 806 cm^{-1} are assigned to the O–W–O modes and the peak at 956 cm^{-1} corresponds to the W=O stretching mode of terminal oxygen, possibly on the surface of the cluster. A similar appearance of the Raman peaks was reported by Daniel *et al* [23] for a monoclinic WO_3 film, which is consistent with our present XRD analysis. It can be mentioned that Salje [24] reported a change in the Raman spectra of crystalline WO_3 to be caused due to a phase transition, although Shigesato *et al* [25] observed that the location of the Raman peak at 807 cm^{-1} is hardly affected due to the structural phase transition. Comparing the Raman spectra of the pristine sample with the irradiated samples, it is clear that the shift in the peak positions is rather insignificant, which suggests that no structural phase transition takes place

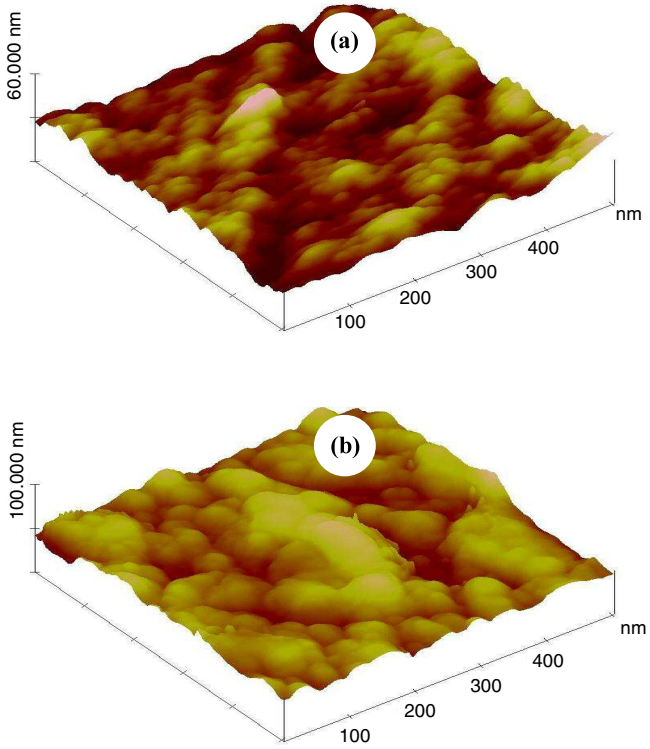

Figure 5. Atomic force microscope images before and after N^+-ion irradiation at various fluences: (a) AFM image (500 nm × 500 nm × 60 nm) corresponding to the pristine WO_3 film; (b) AFM image (500 nm × 500 nm × 100 nm) obtained from a WO_3 film irradiated at a fluence of 1×10^{15} N^+ cm^{-2}.

in the WO_3 films upon ion irradiation. However, the relative intensity (peak height) of the Raman lines decreases with increasing ion fluence, which is similar to the results observed for 6.8 MeV N^+-ion irradiated WO_3 films [13]. This can be interpreted on the basis of the electronic screening of phonons in conjunction with intraband activity within the framework of the proposed band structure in the metallic state [26]. In addition, the Raman peak widths also increase (as shown in figure 3), since the phonon lifetime reduces whenever an increase in the defect density takes place in a lattice.

Kubo and Nishikitani reported that the ratio of integrated Raman scattering intensities of the W=O band to that of the O–W–O band can be employed as a measure of the cluster size, and concluded that the quantity of W=O is inversely proportional to the cluster size [27]. Therefore, a decrease in intensity of the W=O peak with increasing ion fluence may be indicative of increasing grain size of the films, which is clearly seen from figure 1(b).

In order to have a better insight into the role of N-ion irradiation of the WO_3 films, we now try to correlate our Raman data with the other measurements. As a first step, we plot the variation in the area under the different Raman peaks of the WO_3 films (figure 4). It is observed that the area under all the Raman peaks decreases with increasing ion fluence. The area under a Raman line may reduce due to deterioration in the translational symmetry of the WO_3 crystal caused by irradiation induced lattice disorder [28]. This is supported by our XRD measurements, where we observe an irradiation induced distortion in the W–O network. In addition, a reduction in the peak area of different Raman lines is correlated with a decrease in

the optical band gap [29], which is indeed true in our case as well. Further, the optical band gap also shows a tendency to decrease when the W=O:O–W–O ratio reduces [27], which is consistent with our results, yielding a decrease in the E_g value with decreasing intensity of the W=O band.

In addition, the average root mean square (rms) surface roughness of the films increases with ion fluence. For instance, the average rms surface roughness of the pristine sample is 3.7 nm, which increases up to 7.4 nm for the irradiated films at a fluence of 1×10^{15} ions cm^{-2}. This is easily realized by looking at the AFM images shown in figure 5. As pointed out earlier, the effects of 2 MeV N^+ ions would be governed by the electronic excitation, which is responsible for the changes in the irradiated films. Normally, it is expected that the electronic excitation will not cause any movement of atoms because it is typically known to cause either excitation or ionization. However, WO_3 films are insulating in nature and, according to the Coulomb explosion model, the positive charges generated by the incident ion along its path may cause atomic motion due to the Coulomb force [11, 30].

4. Summary and conclusions

In conclusion, we have studied the modifications in the structural, optical, vibrational, and the surface morphological properties of WO_3 thin films irradiated with 2 MeV N^+ ions. We observe irradiation induced grain growth in the films by XRD analysis, although no structural phase transition takes place due to irradiation up to the highest fluence of 1×10^{15} ions cm^{-2}. These observations are corroborated by Raman studies. Optical studies show an increase in the optical absorption and a systematic reduction in the band gap values of the films with increasing ion fluence, which is associated with N-ion induced defects, leading to the production of localized states near the band edges and in the energy gap of WO_3. This trend is further correlated with the Raman studies, where we observe a decreasing intensity of the Raman peak of W=O band with increasing ion fluence.

Acknowledgments

We thank the Pelletron group for providing an uninterrupted beam during the irradiation work. Thanks are due to Dr S N Sahu for extending the Raman scattering and optical absorption facilities. Dr S Varma is acknowledged for extending the AFM facility.

References

[1] Pulker H K 1987 *Coatings on Glass* (New York: Elsevier)
[2] Baucke F G K, Bange K and Gambke T 1988 *Displays* **9** 179
[3] Lampert C M and Granqvist C G (ed) 1990 *Large Area Chromogenics: Materials and Devices for Transmittance Control* (Bellingham, WA: SPIE Optical Engineering)
[4] Granqvist C G 1995 *Handbook of Inorganic Electrochromic Materials* (Amsterdam: Elsevier)
Monk P M S, Mortimer R J and Rosseinsky D R 1995 *Electrochromism: Fundamentals and Applications* (Weinheim: VCH Verlagsgesellschaft)
[5] Granqvist C G 2000 *Sol. Energy Mater. Sol. Cells* **60** 201
Ionescu R, Llobet E, Brezmes J, Vilanova X and Correig X 2003 *Sensors Actuators* B **95** 177
[6] Sivakumar R, Gopalakrishnan R, Jayachandran M and Sanjeeviraja C 2006 *Smart Mater. Struct.* **15** 877
[7] Miyakawa M, Kawamura K, Hosono H and Kawazoe H 1998 *J. Appl. Phys.* **84** 5610
[8] Miyakawa M, Ueda K and Hosono H 2002 *J. Appl. Phys.* **92** 2017
Stankova N E, Atanasov P A, Stanimirova T J, Dikovska A Og and Eason R W 2005 *Appl. Surf. Sci.* **247** 401
[9] Williams J S and Poate J M 1984 *Ion Implantation and Beam Process* (New York: Academic)

Townsend P D, Chandler P J and Zhang L 1994 *Optical Effects of Ion Implantation* (Cambridge: Cambridge University Press)
[10] Ghosh S, Mäder M, Grötzschel R, Gupta A and Som T 2006 *Appl. Phys. Lett.* **89** 104104
[11] Sivakumar R, Sanjeeviraja C, Jayachandran M, Gopalakrishnan R, Sarangi S N, Paramanik D and Som T 2007 *J. Appl. Phys.* **101** 034913
[12] Heinz B, Merz M, Wildmayer P and Ziemann P 2001 *J. Appl. Phys.* **90** 4007
[13] Wagner W, Rauch F, Feile R, Ottermann C and Bange K 1993 *Thin Solid Films* **235** 228
[14] Zeigler J F, Biersack J P and Littmark U 1985 *The Stopping and Ranges of Ions in Solids* vol 1 (New York: Pergamon) http://www.srim.org/
[15] JCPDS-International Center for Diffraction Data 2000 *Powder Diffraction File No.* 83-0950 ICDD, Newton Square, PA
[16] Culity B D 1978 *Elements of X-ray Diffraction* (Philippines: Addison-Wesley)
[17] Williamson G B and Smallman R C 1956 *Phil. Mag.* **1** 34
Gopal S, Viswanathan C, Karunagaran B, Narayandass Sa K, Mangalaraj D and Yi J 2005 *Cryst. Res. Technol.* **40** 557
[18] Ungar T 2004 *Scr. Mater.* **51** 777
[19] Tate T J, Garcia-Parajo M and Green M 1991 *J. Appl. Phys.* **70** 3509
[20] Svensson J S E M and Granqvist C G 1984 *Appl. Phys. Lett.* **45** 828
[21] Madhuri K V, Naidu B S, Hussain O M, Eddrief M and Julien C 2001 *Mater. Sci. Eng.* B **86** 165
[22] Shigesato Y 1991 *Japan. J. Appl. Phys.* **30** 1457
[23] Daniel M F, Desbat B, Lassegues J C, Gerand B and Figlarz M 1987 *J. Solid State Chem.* **67** 235
[24] Salje E 1975 *Acta Crystallogr.* A **31** 360
[25] Shigesato Y, Murayama A, Kamimori T and Matsuhiro K 1988 *Appl. Surf. Sci.* **33/34** 804
[26] Hirata T, Ishioka K and Kitajima M 1996 *Appl. Phys. Lett.* **68** 458
[27] Kubo T and Nishikitani Y 1998 *J. Electrochem. Soc.* **145** 1729
[28] Motooka T and Holland O W 1992 *Appl. Phys. Lett.* **61** 3005
[29] Senthil K, Mangalaraj D, Narayandass Sa K, Hong B, Roh Y, Park C S and Yi J 2002 *Semicond. Sci. Technol.* **17** 97
[30] Fleischer R L, Price P B and Walker R M 1965 *J. Appl. Phys.* **36** 3645